Electronic supplementary information

Multiscale structural regulation of metal-organic framework nanofilm arrays for efficient oxygen evolution reaction

Qianwei Liang,‡[a] Yawen Liu,‡[a] Ziqian Xue,[b] Ziyu Zhao,[a] Guangqin Li*[b] and Jianqiang Hu*[a]

[a.] *School of Chemistry and Chemical Engineering, Key Lab of Fuel Cell Technology of Guangdong Province, South China University of Technology, Guangzhou, 510640, P. R. China. E-mail: jqhusc@scut.edu.cn*

[b.] *MOE Laboratory of Bioinorganic and Synthetic Chemistry, Lehn Institute of Functional Materials, School of Chemistry, Sun Yat-Sen University, Guangzhou, 510275, P. R. China. E-mail: liguangqin@mail.sysu.edu.cn*

‡ Q. Liang and Y. Liu contributed equally to this work.

1. Experimental section

1.1 Chemicals

Nickel nitrate hexahydrate ($Ni(NO_3)_2 \cdot 6H_2O$, 98%), cobalt nitrate hexahydrate ($Co(NO_3)_2 \cdot 6H_2O$, 98%), N,N-dimethylformamide (DMF, 99.5%), terephthalic acid (H_2BDC, 99%), ferrocenecarboxylic acid (Fc, 98%), sodium hydroxide (NaOH) and commercial ruthenium dioxide (RuO_2, 99.9%) were purchased from Aladdin (Shanghai, China) , and used without any further purification. The solutions in present work were prepared by ultra-pure water (>18.0 MΩ·cm).

1.2 Preparation of catalysts

1.2.1 Preparation of NiCoBDC-Fc/NF

Ni foam (NF) was cut into rectangular pieces (3 cm × 2 cm), then it was carefully pretreated complying following steps before each experiment: firstly, ultrasonicated in 3.0 M HCl for 20 min to remove oxide layer on surface, after that NF was successively ultrasonicated in acetone, ethanol and water for 10 min, respectively.

Terephthalic acid (H_2BDC) (1 mmol) and different amount ferrocenecarboxylic acid (Fc) (0.05, 01, 0.15, 0.2, 0.3, 0.4 mmol) were dissolved in 5 mL N,N-dimethylformamide (DMF), then 1 mL 0.4 M NaOH was added under stirring. After that, the solution above was slowly mixed with 5 mL $Ni(NO_3)_2 \cdot 6H_2O$ (0.5 mmol) and $Co(NO_3)_2 \cdot 6H_2O$ (0.5 mmol) DMF solution in a 25 mL Teflon-lined stainless-steel autoclave (Anhui Chem-n Instrument Co., Ltd.), then a piece of NF was put into the autoclave. The Teflon-lined stainless-steel autoclave was sealed and heated at 100°C for 15 h. The resulting electrocatalyst (marked as NiCoBDC-Fc/NF) was washed with DMF and ethanol three times and dried naturally.

1.2.2 Preparation of NiBDC/NF

BDC (1 mmol) was dissolved in 5 mL DMF, then 1 mL 0.4 M NaOH was added under stirring. The solution above was slowly mixed with 5 mL $Ni(NO_3)_2 \cdot 6H_2O$ (1 mmol) DMF solution in a 25 mL Teflon-lined stainless-steel autoclave, then a piece of NF was put into the autoclave. Subsequently, the Teflon-lined stainless-steel

autoclave was sealed and heated at 100°C for 15 h. The resulting electrocatalyst (marked as NiBDC/NF) was washed with DMF and ethanol for three times and dried naturally.

1.2.3 Preparation of NiCoBDC/NF

H_2BDC (1 mmol) were dissolved in 5 mL DMF, then 1 mL 0.4 M NaOH was added under stirring. The solution above was slowly mixed with 5 mL $Ni(NO_3)_2 \cdot 6H_2O$ (0.5 mmol) and $Co(NO_3)_2 \cdot 6H_2O$ (0.5 mmol) DMF solution in a 25 mL Teflon-lined stainless-steel autoclave, then a piece of NF was put into the autoclave. After that, the Teflon-lined stainless-steel autoclave was sealed and heated at 100°C for 15 h. The resulting electrocatalyst (marked as NiCoBDC/NF) was washed with DMF and ethanol for three times and dried naturally. Ni_xCo_yBDC/NF with different metal ratios were synthesized in the similar process and controlling the same total metal and ligand content, and the feeding ratios of Ni:Co as 9:1, 3:1, 1:1 and 1:3.

1.2.4 Preparation of RuO_2/NF

The commercial RuO_2 (10 mg) was dispersed into a mixture of 980 μL ethanol and 20 μL Nafion (5%), and the mixture was ultrasonicated for 30 min to form homogeneous ink. Then, a certain amount ink was loaded onto nickel foam and dried at room temperature. The loading amount of RuO_2 on the NF is about 2.5 $mg \cdot cm^{-2}$, which is the same loading mass with prepared electrocatalyst.

1.3 Characterization

The morphology and structure of the samples were characterized by scanning electron microscopy (SEM, Hitachi SU8010, 5kV) and transmission electron microscopy (TEM, JEOL, JEM-1400, 120 kV). The crystallinity and purity of the materials was evaluated qualitatively by thin film powder X-ray diffraction (XRD, Bruker, D8 Advance, Germany) equipped with a Cu Kα radiation source (λ=1.5406 Å), and the test conditions were set as 2θ range from 5° to 50° at scanning rate of $5° \cdot min^{-1}$. The N_2 adsorption-desorption isotherms were collected using a Micromeritics Instrument (ASAP 2460, America) at 77 K. The surface properties of

the products were analyzed with X-ray photoelectron spectroscopy (XPS, Nexsa, Thermo Fisher Scientific, America) with a Mg Kα X-ray source. The content of Co, Ni and Fe in different specimens was determined by inductively couple plasma-mass spectrometer (ICP-MS, iCAP Qc, Thermo Fisher Scientific).

1.4 Electrochemical measurements

Electrochemical measurements were performed on a CHI 760E electrochemistry workstation with a three-electrode system. The Ag/AgCl and platinum plate electrode were used as the reference and counter electrode, respectively. The as-prepared catalysts on NF were used as working electrodes. The measured potentials were converted to reversible hydrogen electrode (RHE), $E_{RHE} = E_{Ag/AgCl} + 0.21 + 0.059 \times pH$. Linear sweep voltammetry (LSV) curves were recorded in 1.0 M KOH aqueous solutions with 95% *iR*-compensation at a scan rate of 2 $mV \cdot s^{-1}$. Tafel slopes were calculated by linear regression using the equation $\eta = b \cdot \log|j| + a$, where η (V) is the overpotential, j is the current density ($mA \cdot cm^{-2}$), respectively. The electrochemically active surface areas (ECSA) were investigated by double-layer capacitance (C_{dl}) in the potential range from 0-0.1 V vs. $E_{Ag/AgCl}$ with different scan rates (20, 40, 80, 120，160 and 200 $mV \cdot s^{-1}$). The electrochemical impedance spectroscopy (EIS) was measured in 1.0 M KOH aqueous solutions with a frequency range from 10^5 to 0.01 Hz at 1.45 V vs. RHE.

2. Supplementary figures

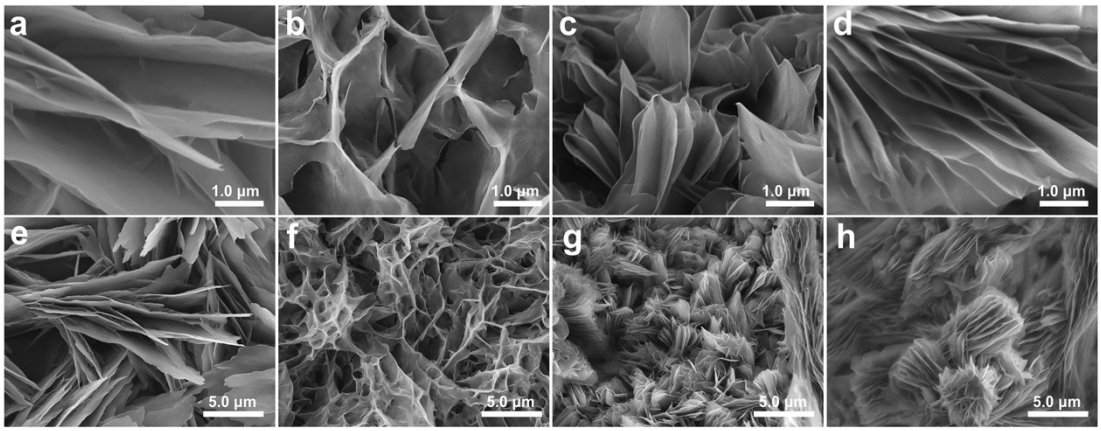

Fig. S1 SEM images of NiCoBDC/NF in different metal ratio (a,e) $NiCo_{0.12}BDC/NF$; (b,f) $NiCo_{0.35}BDC/NF$; (c,g) $NiCo_{1.09}BDC/NF$; (d,h)$NiCo_{2.85}BDC/NF$.

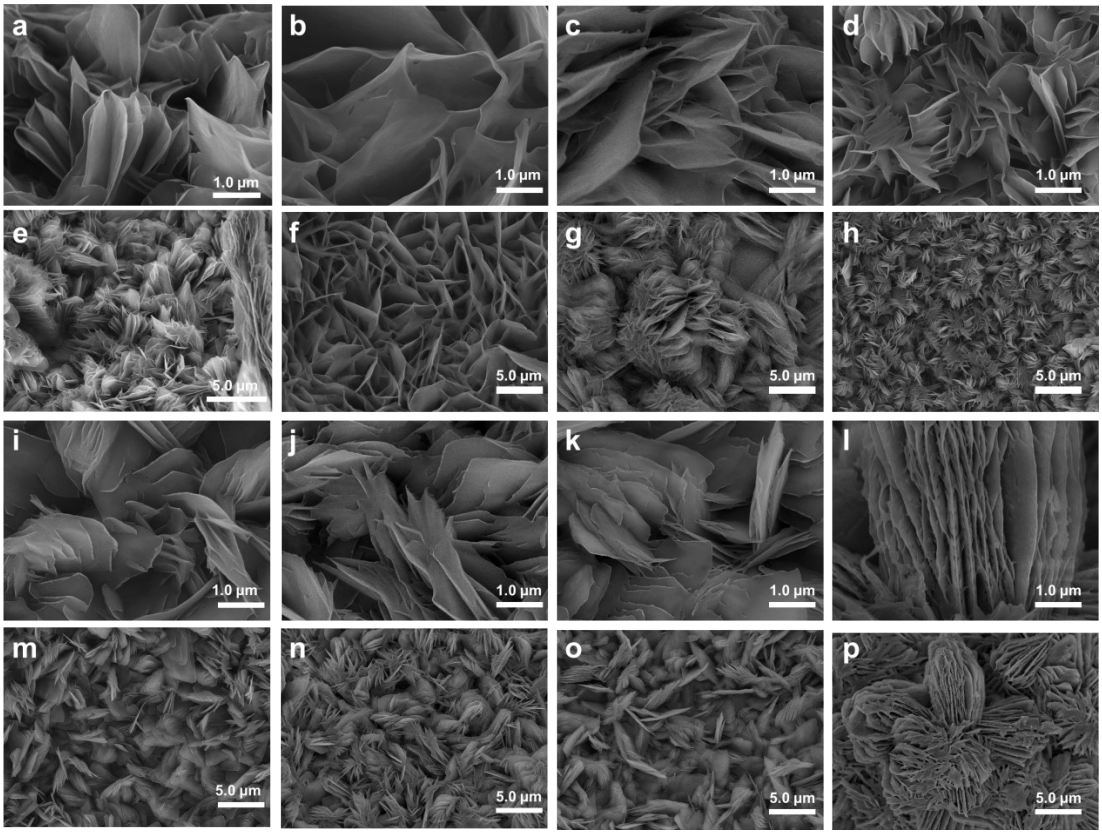

Fig. S2 SEM images of NiCoBDC-Fc/NF in different metal ratio (a,e) NiCoBDC/NF, (b,f) $NiCo_{1.09}BDC\text{-}Fc_{0.07}/NF$, (c,g) $NiCo_{1.14}BDC\text{-}Fc_{0.11}/NF$, (d,h) $NiCo_{1.16}BDC\text{-}Fc_{0.14}/NF$, (i,m) $NiCo_{1.13}BDC\text{-}Fc_{0.17}/NF$, (j,n) $NiCo_{1.09}BDC\text{-}Fc_{0.25}/NF$, (k,o) $NiCo_{1.15}BDC\text{-}Fc_{0.30}/NF$, (l,p) $NiCo_{1.11}BDC\text{-}Fc_{0.35}/NF$.

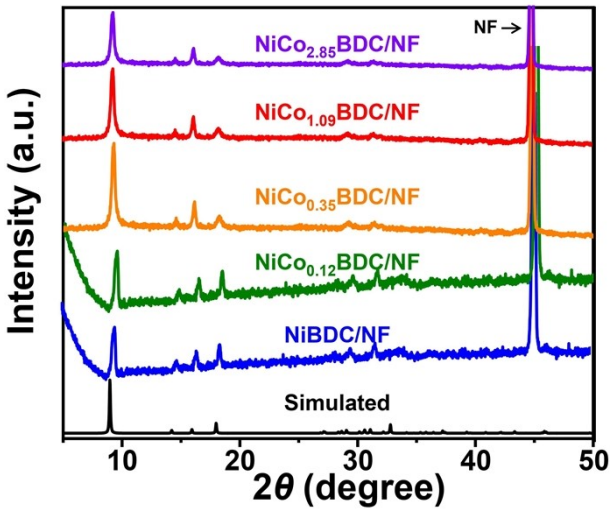

Fig. S3 Comparison of XRD patterns of NiCoBDC/NF in different metal ratio.

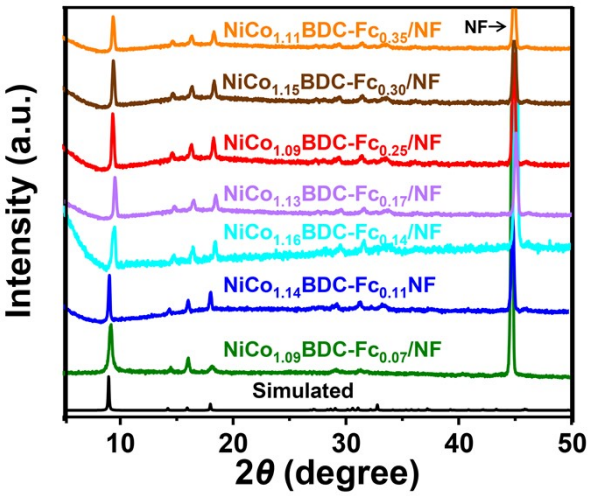

Fig. S4 Comparison of XRD patterns of NiCoBDC-Fc/NF in different metal ratio.

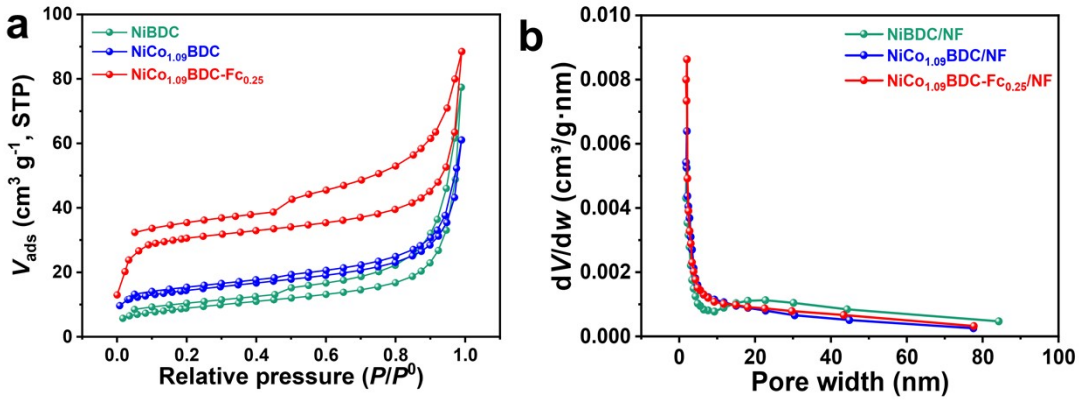

Fig. S5 (a) N_2 absorption/desorption isotherms, (b) Pore size distribution curves of electrocatalysts.

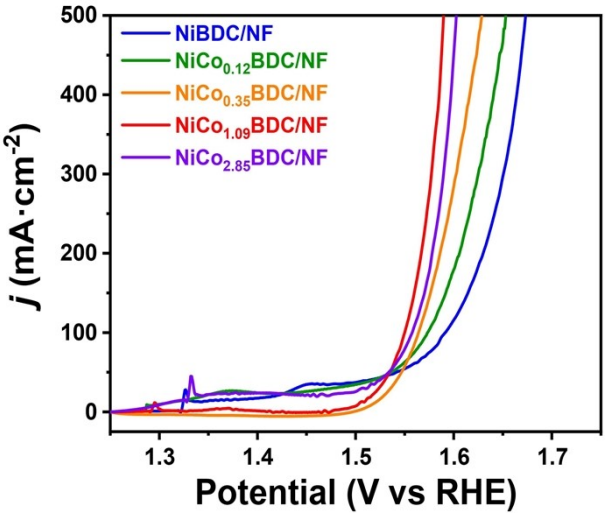

Fig. S6 OER performances of different catalysts in 1.0 M KOH.

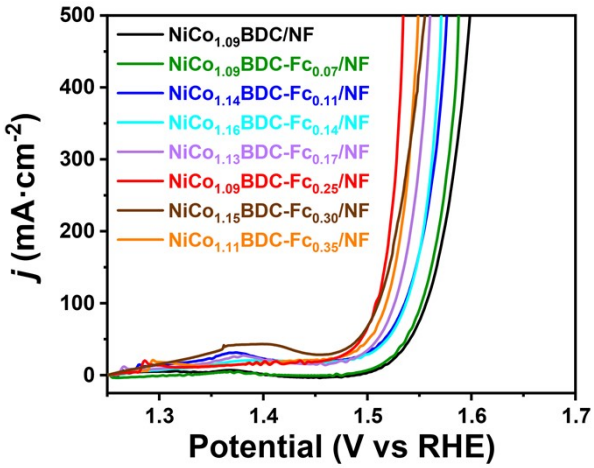

Fig. S7 OER performances of different catalysts in 1.0 M KOH.

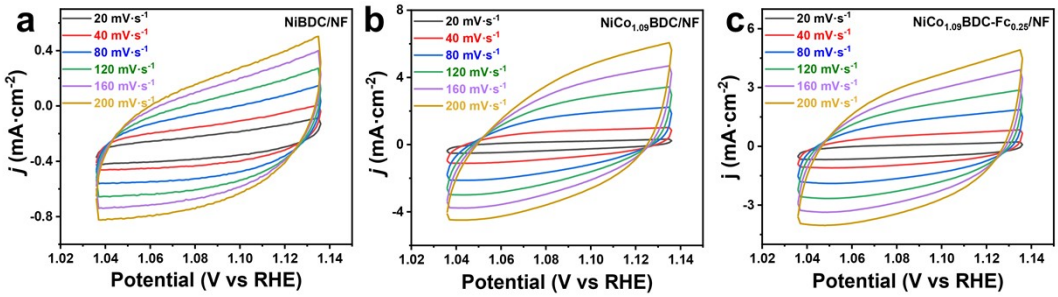

Fig. S8 CV plots of (a) NiBDC/NF, (b) $NiCo_{1.09}BDC/NF$, (c) $NiCo_{1.09}BDC\text{-}Fc_{0.25}/NF$ at different scan rates, (d) capacitive currents as a function of the scan rate to give the double-layer capacitance (C_{dl}) for different catalysts.

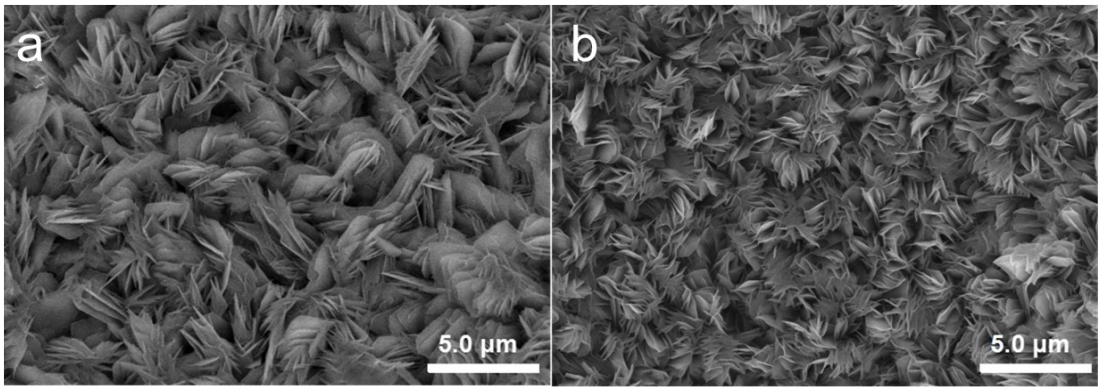

Fig. S9 SEM images of $NiCo_{1.09}BDC\text{-}Fc_{0.25}$ (a) before and (b) after stability test.

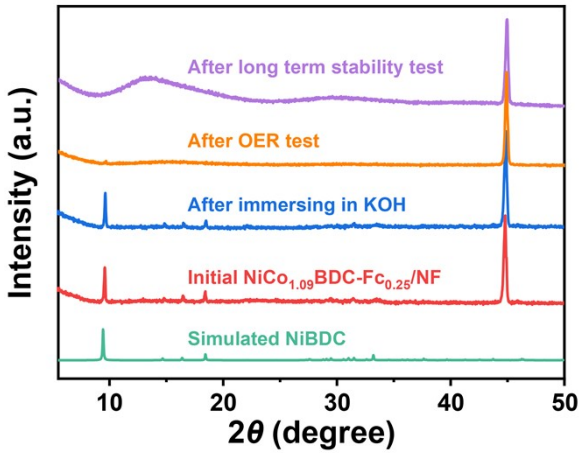

Fig. S10 XRD patterns of initial $NiCo_{1.09}BDC\text{-}Fc_{0.25}$ and after immersing in KOH, OER test and stability test.

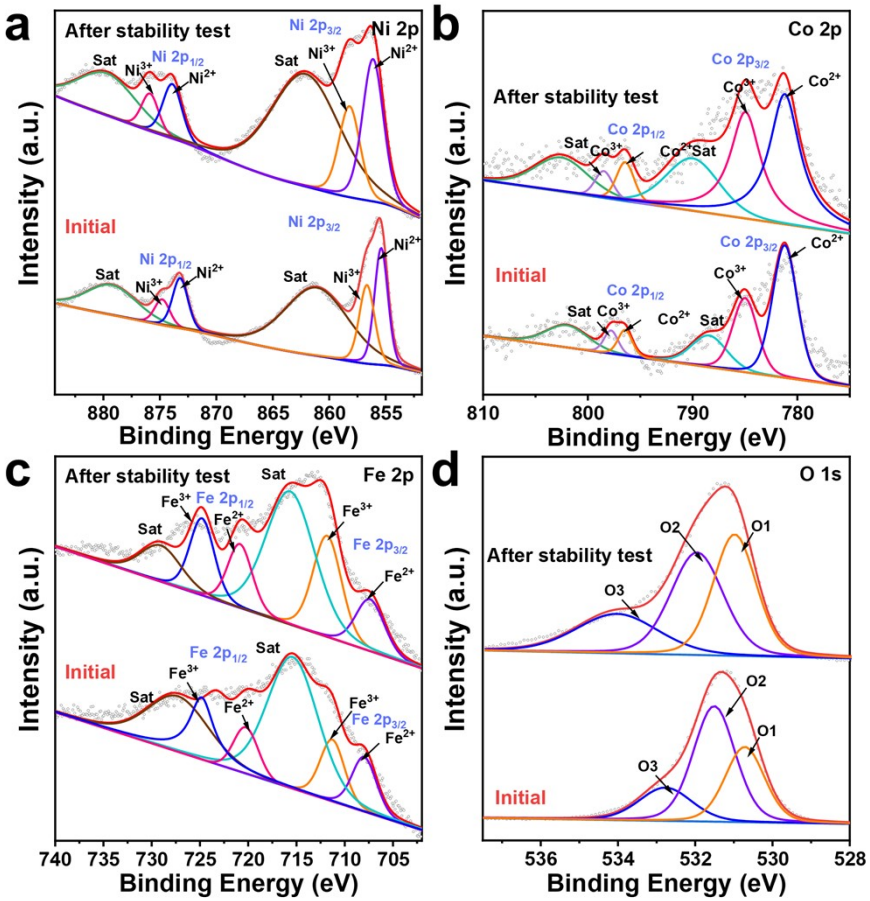

Fig. S11 (a) Ni 2p XPS spectra, (b) Co 2p XPS spectra, (c) Fe 2p XPS spectra, (d) O 1s XPS spectra of $NiCo_{1.09}BDC\text{-}Fc_{0.25}$ before and after stability test in 1.0 M KOH.

Table S1 ICP-MS results of NiCoBDC/NF.

Catalyst	The molar ratio of precursor Ni:Co	Mass ratio		Atom%	
		Ni	Co	Ni	Co
$NiCo_{0.12}BDC/NF$	9:1	1.00	0.12	89.32	10.68
$NiCo_{0.35}BDC/NF$	3:1	1.00	0.35	74.15	25.85
$NiCo_{1.09}BDC/NF$	1:1	1.00	1.09	47.95	52.05
$NiCo_{2.85}BDC/NF$	1:3	1.00	2.85	25.99	74.01

Table S2 ICP-MS results of NiCoBDC-Fc/NF.

Catalyst	The amount of precursor Fc (mmol)	Mass ratio			Atom%		
		Ni	Co	Fe	Ni	Co	Fe
$NiCo_{1.09}BDC\text{-}Fc_{0.07}/NF$	0.05	1.00	1.09	0.07	46.31	50.28	3.41
$NiCo_{1.14}BDC\text{-}Fc_{0.11}/NF$	0.10	1.00	1.14	0.11	44.63	50.68	4.69
$NiCo_{1.16}BDC\text{-}Fc_{0.14}/NF$	0.15	1.00	1.16	0.14	43.63	50.41	5.96
$NiCo_{1.13}BDC\text{-}Fc_{0.17}/NF$	0.20	1.00	1.13	0.17	43.60	49.07	7.33
$NiCo_{1.09}BDC\text{-}Fc_{0.25}/NF$	0.30	1.00	1.09	0.25	42.78	46.44	10.79
$NiCo_{1.15}BDC\text{-}Fc_{0.30}/NF$	0.35	1.00	1.15	0.30	40.81	46.75	12.44
$NiCo_{1.11}BDC\text{-}Fc_{0.35}/NF$	0.40	1.00	1.11	0.35	40.78	45.08	14.14

Table S3 Comparisons of OER activity of art non-noble-metal electrocatalysts.

Catalyst	Overpotential (mV)	Tafel slope (mV dec^{-1})	Substrates	Refs.
$NiCo_{1.09}BDC\text{-}Fc_{0.25}/NF$	η_{50}=263 η_{100}=278	43	Ni foam	**This work**
NiCo-MOF/NF	η_{50}=270	35	Ni foam	1
MoCoNiS/NF	η_{100}=226	45	Ni foam	2
FeMn-MOF/NF	η_{50}=290	87	Ni foam	3
MIL-53(Co-Fe)/NF	η_{100}=262	69	Ni foam	4
$NiFe_3Nb_2$-OH	η_{100}=294	47	Ni foam	5
Co-Ni-Fe-P HNBs	η_{50}=303	59	carbon paper	6
$CoNiFeO_x$-NC	η_{50}=263	64	carbon paper	7
Ni-Fe-Al-Co LDHs	η_{100}=220	29	carbon fiber cloth	8
$(Ni,Co)S_2$	η_{10}=270	58	carbon fiber cloth	9
EG/$(Co,Ni)Se_2$-NC	η_{10}=258	73	graphite foil	10
Co-Ni_3C/Ni@C	η_{10}=325	68	GCE	11
Co-Ni-O_x/BG	η_{10}=310	55	GCE	12
CoZn MOF/CC	η_{10}=287	76	GCE	13
$Ni_{0.25}Co_{0.75}(OH)_2$	η_{10}=352	72	GCE	14
$(Fe(II)_1Fe(III)_1)_{0.6}$ /NMOF-Co	η_{10}=230	50	GCE	15

References

[1] P. Thangasamy, S. Shanmuganathan, V. Subramanian, *Nanoscale Advances* **2020**, 2, 2073-2079.

[2] J.F. Qin, M. Yang, T.-S. Chen, B. Dong, S. Hou, X. Ma, Y.-N. Zhou, X.-L. Yang, J. Nan, Y.-M. Chai, *International Journal of Hydrogen Energy* **2020**, 45, 2745-2753.

[3] H. Guan, N. Wang, X. Feng, S. Bian, W. Li, Y. Chen, *Colloids and Surfaces a-Physicochemical and Engineering Aspects* **2021**, 624.

[4] M. Xie, Y. Ma, D. Lin, C. Xu, F. Xie, W. Zeng, *Nanoscale* **2020**, 12, 67-71.

[5] J. Pan, S. Hao, X. Zhang, R. Huang, *Inorganic Chemistry Frontiers* **2020**, 7, 3465-3474.

[6] Y. Wang, L. Sun, L. Lu, D. Xu, Q. Hao, B. Liu, *Journal of Materials Chemistry A* **2021**, 9, 3482-3491.

[7] C. Chen, Y. Tuo, Q. Lu, H. Lu, S. Zhang, Y. Zhou, J. Zhang, Z. Liu, Z. Kang, X. Feng, D. Chen, *Applied Catalysis B-Environmental* **2021**, 287.

[8] E. Enkhtuvshin, K.M. Kim, Y.-K. Kim, S. Mihn, S.J. Kim, S.Y. Jung, N.T.T. Thao, G. Ali, M. Akbar, K.Y. Chung, K.H. Chae, S. Kang, T.W. Lee, H.G. Kim, S. Choi, H. Han, *Journal of Materials Chemistry A* **2021**.

[9] J. Zhang, X. Bai, T. Wang, W. Xiao, P. Xi, J. Wang, D. Gao, J. Wang, *Nano-Micro Letters* **2019**, 11.

[10] J. Cao, K. Wang, J. Chen, C. Lei, B. Yang, Z. Li, L. Lei, Y. Hou, K. Ostrikov, *Nano-Micro Letters* **2019**, 11.

[11] X. Jia, M. Wang, G. Liu, Y. Wang, J. Yang, J. Li, *International Journal of Hydrogen Energy* **2019**, 44, 24572-24579.

[12] Y. Jiang, K. Dong, Y. Lu, J. Liu, B. Chen, Z. Song, L. Niu, *Science China-Materials* **2020**, 63, 1247-1256.

[13] J. Wu, Z. Yu, Y. Zhang, S. Niu, J. Zhao, S. Li, P. Xu, *Small* **2021**.

[14] Y. Wang, C. Yang, Y. Huang, Z. Li, Z. Liang, G. Cao, *Journal of Materials Chemistry A* **2020**, 8, 6699-6708.

[15] M. Zhao, T. Guo, W. Qian, Z. Wang, X. Zhao, L. Wen, D. He, *Chemical Engineering Journal* **2021**, 422.